Preclinical zebrafish model for organophosphorus intoxication: neuronal hyperexcitation, behavioral abnormalities and subsequent brain damages

Alexandre Brenet[1], Julie Somkhit[1], Rahma Hassan-Abdi[1], Constantin Yanicostas[1], Alexandre Igert[2], Dominique Saurat[3], Nicolas Taudon[3], Roxane Loyant[4], Mathieu Porceddu[4], Gregory Dal-Bo[2], Florian Nachon[2], Nina Dupuis[2#], and Nadia Soussi-Yanicostas[1#]*

[1] Université de Paris, NeuroDiderot, Inserm, F-75019 Paris, France

[2] Institut de Recherche Biomédicale des Armées (IRBA), Département de toxicologie et risques chimiques, F-91 220 Brétigny-sur-Orge, France.

[3] Institut de Recherche Biomédicale des Armées (IRBA), Unité de développements analytiques et bioanalyse, F-91 220 Brétigny-sur-Orge, France.

[4] Mitologics SAS, Faculté de Médecine, 94000 Créteil, France

# These authors contributed equally to this work.

* Corresponding authors:

Dr Nadia Soussi-Yanicostas
Neurodiderot
INSERM U1141
48 boulevard Serurier
75019 Paris
France
e-mail : nadia.soussi@inserm.fr
phone : +33 (0)1 40 03 19 31

ABSTRACT

As key compounds for modern cultivation practices, organophosphorus (OP)-containing pesticides have become an important public health and environmental issues, worldwide, causing millions human intoxications each year. OP poisoning induces cholinergic syndrome, associating irreversible brain damages with epileptic seizures, possibly ending in life-threatening status epilepticus. Existing countermeasures are life-saving, but insufficiently effective to prevent long lasting neuronal consequences, emphasizing the dire need for animal models mimicking OP poisoning as tools to identify novel anti-OP countermeasures. Here, we used diisopropylfluorophosphate (DFP), a prototypic and moderately toxic OP compound, to generate a zebrafish OP intoxication model and study the consequences of DFP exposure on neuronal activity, larvae behaviour and neuron network organization. DFP poisoning caused marked acetylcholinesterase (AChE) inhibition, resulting in paralysis, decreased oxygen consumption, overexpression of c-Fos neuron activity marker, increased neuron apoptosis and epileptiform seizure-like activity, which was partially alleviated by diazepam treatment. DFP-exposed larvae also showed altered neuron networks with increased accumulation of NR2B-NMDA receptor combined with decreased GAD65/67 and gephyrin protein accumulation. Thus, we described a zebrafish model of DFP poisoning, which should (i) provide important insights into the pathophysiological mechanisms underlying OP intoxication and ensuing brain damage, and (ii) help identify novel therapeutic agents to restore CNS functions following acute OP poisoning.

KEYWORDS: Zebrafish model; Organophosphorus (OP) intoxication; Epileptiform seizure; Neuron toxicity, Diisopropylfluorophosphate (DFP); Respiratory failure.

1. INTRODUCTION

Organophosphorus (OP) compounds are highly toxic molecules used as lethal weapons in both war situations and terrorist attacks, but also as key chemical pesticides to combat pests and parasites. As the result of their massive use for agricultural purposes worldwide, OP poisoning represents today a major public health issue with 3 million severe intoxications reported annually and more than 200,000 deaths, primarily suicides[1–4]. OP are potent inhibitors of cholinesterase, including acetylcholinesterase (AChE), causing massive acetylcholine accumulation at cholinergic synapses and overstimulation of cholinergic receptors at both neuromuscular junctions and CNS cholinergic synapses[5]. OP-induced cholinergic hyperactivity in the brain can provoke epileptic seizures, which, if not rapidly treated, may turn into life-threatening status epilepticus[6]. Besides immediate toxicity, survivors of OP poisoning also face long-term comorbidities that include psychomotor defects, cognitive deficits and recurrent seizures[7,8]. Existing countermeasures against OP poisoning are life-saving but not yet sufficiently effective against seizure occurrence and brain damage. There is thus an urgent need for new therapeutic agents.

The generation and characterization of an animal model of OP intoxication faithfully mimicking the consequences of OP poisoning in humans is urgently needed both for a better understanding of OP poisoning pathophysiology and for high-throughput screening of therapeutic entities counteracting the toxicity of these compounds. Rodent OP intoxication models are not fully pure, because respiratory blockade induced by OP requires mandatory co-administration of both cholinergic agonist and AChE reactivator with the tested OP compounds. As an alternative vertebrate species, we describe here a preclinical zebrafish model of OP poisoning and characterize the neuron defects induced.

Over the past decade, besides its skyrocketing use as a human disease model [9–13], the zebrafish has become one of the leading animal models for toxicology research[14]. This small and easy-to-breed fish offers significant advantages for in vivo drug discovery and neurotoxicology investigations, including a CNS that displays an overall organization similar to that of mammals and full conservation of different neuron types, neurotransmitters and glial cell types[15–19].

To model OP intoxication in zebrafish, we used diisopropylfluorophosphate (DFP), an analogue of the chemical warfare agents sarin and soman, which promotes potent AChE inhibition. However, DFP is safer, less volatile, and much less dangerous for experimentation purposes than soman, making it an OP fully suited to experimental research. It has been shown that acute DFP intoxication in rats induces seizures[20] and causes neurodegeneration, memory impairment and neuroinflammation[20,21]. DFP has been used to model seizures with subsequent behavioral deficits in rodents[22–25]. However, while it has long been known that acute intoxication with OP nerve agents, such as sarin, soman and DFP, causes neuropathological changes in the brain in both human patients and animal models[8,21,26,27], this brain damage and its extent remain poorly understood.

By combining behavioral analysis, respiration measurements, in vivo brain calcium imaging and molecular and immunocytochemical approaches, we showed that larvae exposed to DFP displayed motor paralysis correlated with inhibition of AChE activity and depressed respiration. DFP-treated larvae also showed increases in both c-Fos expression and neuronal calcium uptakes, which reflect epileptiform seizures. We also observed a marked increase in neuron apoptosis and excitatory NR2B-NMDA receptor sub-unit accumulation, combined with a decreased accumulation of both GAD65/67 and gephyrin proteins, reflecting a shift of the synaptic balance toward excitatory states.

2. MATERIALS AND METHODS

2.1 Fish husbandry and zebrafish lines

Zebrafish were kept at 26–28 °C in a 14 h light/10 h dark cycle. Embryos were collected by natural spawning and raised in E3 solution at 28.5 °C. To inhibit pigmentation, 0.003% 1-phenyl-2-thiourea was added at 1 day post-fertilization (dpf). Tg[HuC:GCaMP5G] transgenic line was used to monitor calcium activity, otherwise wild-type AB embryos were used. All the animal experiments were conducted at the French National Institute of Health and Medical Research (INSERM) UMR 1141 in Paris in accordance with European Union guidelines for the handling of laboratory animals (http://ec.europa.eu/environment/chemicals/lab_animals/home_en.htm), and were approved by the Direction Départementale de la Protection des Populations de Paris and the French Animal Ethics Committee under reference No. 2012-15/676-0069.

2.2 DFP treatment

Diisopropylfluorophosphate (DFP) was purchased from Sigma Aldrich. A stock solution (5.46 mM), stored at -20°C, was diluted extemporaneously to 15 μM in 1% DMSO. Control zebrafish larvae were treated with 1% DMSO.

2.3 DFP stability

Ranging amounts of DFP were diluted in 1% DMSO, and 200 μL water samples were removed at different incubation times (0, 2, 4, 6 and 24 h; n = 3 per condition) and were stored at -20 °C until extraction. 360 μL of ethyl acetate (VWR) was added to 180 μL of the sample. After vigorous shaking, an aliquot (100 μL) of organic phase was extracted (recovery > 90%) and stored

at 4 °C until analysis by gas chromatography-mass spectrometry (GC-MS). GC-MS analyses were conducted with a gas chromatograph (Agilent 6890N) coupled to a quadrupole mass spectrometer equipped with an EI source (Agilent MSD5973). After a pulsed splitless injection (40 psi) at 220 °C, the GC separation was performed on an Rtx-OPP2 column (Restek, 30 m x 0.25 mm x 0.25 μm) using a linear ramp from 40 °C to 280 °C (20 °C/min). The mobile phase was helium (99.9995%) at a flow rate of 1.2 mL/min. The source and quadrupole temperatures were set at 230 °C and 150 °C. Acquisition was performed in the SIM (single ion monitoring) mode (m/z 101 and 127 as quantifier and qualifier ions). Operating software was MassHunter Workstation Quantitative analysis version B.09.00/Build 9.0.647.0. DFP concentrations were calculated based on a linear calibration curve (individual residuals within ±20%), obtained with solutions of DFP in ethyl acetate between 0.05 and 1.35 μg/mL.

2.4 Acetylcholinesterase activity

Five dpf zebrafish larvae (20 larvae per sample) were collected at 2 h, 4 h, 6 h post-exposure to DFP and stored at −80 °C for further analysis. Samples were homogenized in 50 mM phosphate buffer (pH 7.4)/0.5% Tween using Precellys® homogenizer with 1.4 mm ceramic beads and centrifuged at 10,000 × g (4 °C) for 10 min. The resulting supernatants were collected and stored at −80 °C. Total protein concentrations were determined using the DC Protein Assay (Bio-Rad) and all the samples were diluted to 1.2 mg/mL. AChE activity was determined by adding 1 mM acetylthiocholine (Sigma) and 0.22 mM 5,5′-dithiobis-2-nitrobenzoic acid (DTNB, Sigma) to the sample (0.03 mg/mL of total proteins), the formation of the product resulting from the reaction between thiocholine and DTNB at 25 °C was monitored for 30 min at 412 nm with a microplate

reader. All the samples were assayed in duplicate. The final results were expressed as percentages of average control activity.

2.5 Measurement of oxygen consumption

Five dpf larvae were exposed to DFP or vehicle (1% DMSO) for 4.5 h and then transferred to 96-well microplates (Greiner Bio-One International) (7 individuals per well) containing 90 μL of E3 medium and 10 μL of 35 μg/mL MitoXpress Xtra (MitoXpress Xtra Reagent Pack, Agilent Technologies) that enables real-time measurement of extracellular oxygen consumption in living larvae. A volume of 100 μL of mineral oil (MitoXpress Xtra Reagent Pack, Agilent Technologies) was added to seal the wells and isolate the reaction medium from ambient air oxygen. Oxygen consumption was then measured in real time for 90 min at 28 °C in a 96-well plate using a spectrofluorimeter (Tecan Spark: $\lambda_{excitation}$ 380 nm, $\lambda_{emission}$ 650 nm). The areas under the linear portion of the curve were used to determine O_2 consumption rates.

2.6 Hematoxylin/eosin staining

Five dpf larvae were exposed to DFP or vehicle (1% DMSO) and then anesthetized using 0.01% tricaine, fixed with 10% formaldehyde, paraffin-embedded and sectioned. Sections were deparaffinized and rehydrated before hematoxylin and eosin staining. Freshly stained sections were treated with ethanol and xylene, and then mounted in Pertex medium. Sections were imaged using a Nikon Eclipse microscope (E-200) equipped with a digital sight (Nikon).

2.7 Zebrafish larval locomotor activity

Locomotor activity of 5 dpf zebrafish larvae was performed as previously described in Brenet et al, 2019[11].

2.8 RT-qPCR

For RNA isolation, larvae were homogenized using a syringe equipped with a 26G needle (seven larvae per sample) using the RNA XS Plus kit (Qiagen, Hilden, Germany). cDNA was synthesized using the iScriptTM cDNA Synthesis Kit (Bio-Rad, Munich, Germany) and qPCR was performed using iQTM SYBR Green Supermix (Bio-Rad). Samples were run in triplicate. Expression levels were normalized to that of eef1a1. The primers (Eurofins Genomics, Ebersberg, Germany) used were: c-fos-forw, 5'-AAC CAG ACT CAG GAG TTC AC-3'; c-fos-rev, 5'-GGA GAA AGC TGT TCA GAT CTG-3'; ee1fa1-forw, 5'-CCA CTA CGA CTG GTC ACC TC-3'; and ee1fa1-rev, 5'-AAG CTT GTC CAG AAC CCA GG-3'.

2.9 Neuronal calcium uptake imaging

Calcium imaging of 5 dpf zebrafish larvae was performed as previously described in Brenet et al, 2019[11].

2.10 Diazepam treatment

Five dpf Tg[Huc:GCaMP5G] larvae were exposed to 15 μM DFP for 5 h and then pancuronium-paralyzed and embedded in 1.1% low-melting agarose in the center of a 35 mm glass-bottomed dish covered with E3 solution containing 300 μM pancuronium bromide. Calcium uptakes were recorded for 30 min prior to diazepam (40 μM DZP, Sigma) addition and calcium

169 activity was then monitored for an additional hour. Calcium activity was measured as described in
170 Brenet et al, 2019[11].

171 **2.11 Apoptosis labeling**

172 Neuronal cell death was visualized and quantified as previously described in Brenet et al,
173 2019[11].

174 **2.12 Immunohistochemistry**

175 For synapse protein immunostaining, zebrafish larvae were fixed using 4% formaldehyde,
176 then directly immersed in 10% sucrose at 4 °C and incubated overnight, embedded in 7.5%
177 gelatin/10% sucrose solution, flash frozen in isopentane at -45 °C and stored at -80 °C until use.
178 When needed, frozen embedded zebrafish larvae were cut into 20 μm cryostat sections, which were
179 mounted on superfrost slides. Sections were then washed, blocked and permeabilized with 0.2%
180 gelatin/0.25% Triton X-100 diluted in PBS. Sections were incubated overnight at room temperature
181 with either anti-gephyrin antibodies (1:100, rabbit polyclonal, Abcam, Ab185993), anti-NR2B-
182 NMDA antibodies (1:200, rabbit polyclonal, Abcam, Ab35677), or anti-GAD65/67 antibodies
183 (1:500, rabbit polyclonal, Abcam, Ab11070). Sections were then washed three times in PBS (5 min
184 each time) and incubated for 2 h at room temperature, in the dark, with an anti-rabbit IgG
185 conjugated with Alexa 488 fluorophore (1:500, mouse, Molecular Probes, A-21206). Sections were
186 finally counterstained for 10 min with 0.3% DAPI, and after a final wash, sections were mounted
187 in Fluoromount medium and stored at 4 °C.

188 **2.13 Synapse quantification**

Sections hybridized with anti-gephyrin antibodies were imaged at full resolution (voxel size: 0.063 x 0.063 x 0.4 μm) using an inversed Leica TCS SP8 confocal scanning system (Leica Microsystems) equipped with an oil-immersion objective (Leica 40x HCPL APO CS2, numerical aperture 1.30). Images were then processed with AutoQuant 3X software (Media Cybernetics) and the density of post-synaptic puncta was quantified using a homemade ImageJ macro (Zsolt Csaba, Inserm UMR1141). After applying a median filter on all images, a threshold was applied to quantify only post-synaptic puncta. Areas of interest that comprised the optic tectum and telencephalon were selected and all spots with sizes in the range 0.018–3.14 μm^2 were considered as post-synaptic puncta. Post-synaptic density of gephyrin puncta was finally calculated by dividing the number of puncta detected in a given region by the surface of the region. Images from four independent experiments were used to calculate mean gephyrin density and corresponding standard error of the mean (SEM), and to assess the statistical significance of the differences observed between DFP-treated and control larvae.

2.14 Quantification of GAD65/67 and NR2B accumulation

Following GAD65/67 and NR2B (NR2B-NMDA) immunostaining, images of brain sections were acquired using an inversed Leica TCS SP8 confocal scanning system (Leica Microsystems) equipped with an oil-immersion objective (Leica 40x HCPL APO CS2, numerical aperture 1.30). Images were acquired in three dimensions (48.50 x 48.50 x 20 μm) and the volume occupied by stained structures was determined using MeasurementPro's Surfaces of the Imaris software (Bitplane Inc., Version 9.1.2). For both GAD65/67 and NR2B/NMDA, images from three independent experiments were used to calculate mean GAD65/67 and NR2B staining volumes and

corresponding standard errors of the mean (SEM), and to assess statistical significance of the differences observed between DFP-treated and control larvae.

3 RESULTS

3.1 Larvae exposed to DFP showed paralysis and acetylcholinesterase (AChE) inhibition

Prior to the development of a zebrafish model of DFP poisoning, we first measured the stability of this compound after dilution in fish water. Ranging amounts of DFP were diluted in fish water and DFP concentrations were determined until 6 hours. Results showed that diluted DFP was stable in fish water, with an average 2% loss per hour, approximately (Figure S1). Next, to determine in vivo DFP toxicity in zebrafish, 5 days post-fertilization (dpf) larvae were exposed to 15, 20, 30, and 50 μM DFP and studied over a 24 h period. Results showed that all larvae incubated in 20 μM DFP or in higher concentration, either died prior to 6 h exposure or displayed gross phenotypic defects, including a curly tail and marked reductions of the head's and eyes' volumes (Figure S2). As we sought to investigate DFP neurotoxicity and subsequent brain damages, we selected 15 µM DFP and an exposure time of 6 h (Figure 1B), an experimental setup that did not induce any visible phenotype (n = 20) when compared to control larvae exposed to 1% DMSO (n = 20) (Figure 1C), nor any significant increase in larvae lethality. Histopathological analysis confirmed that larvae exposed to 15 μM DFP showed no visible neurological abnormalities (Figure S3).

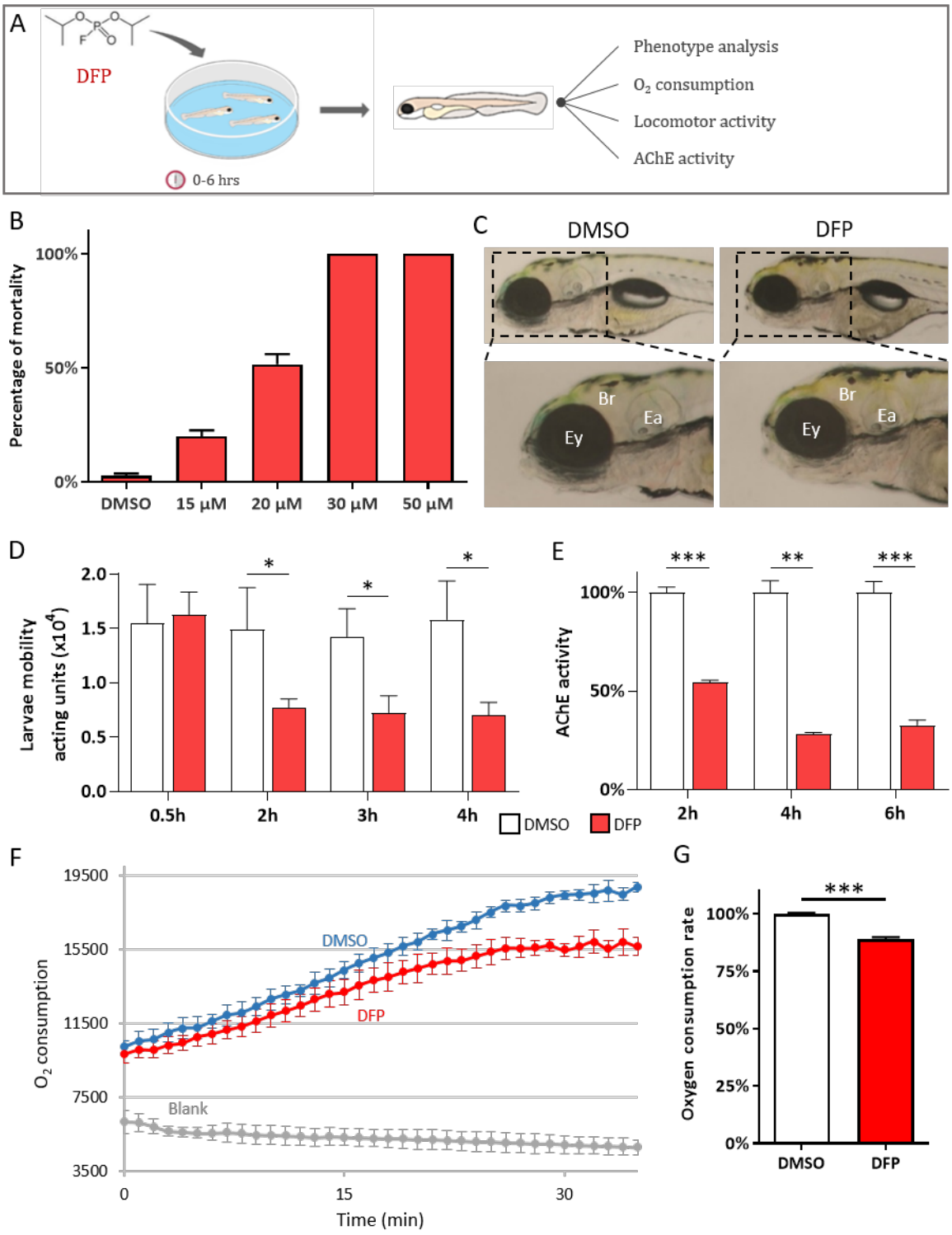

228

229 **Figure 1.** DFP-exposed zebrafish larvae displayed reduced motility, AChE inhibition and

230 respiratory failure. **A**: In the experimental set-up, 5 dpf larvae were exposed to 15, 20, 30 and 50

μM DFP, and larvae lethality, phenotypic defects, locomotor activity and AChE activity were studied for 6 h. **B**: Lethality rates of 5 dpf larvae exposed for 6 h to 15, 20, 30 and 50 μM DFP led us to select 15 μM DFP as optimal concentration (LC20). **C**: 5 dpf larvae exposed for 6 h to either 15 μM DFP or vehicle (DMSO), are phenotypically indistinguishable. **D**: Quantification of AChE activity in larvae exposed to either 15 μM DFP (n = 5) or vehicle (DMSO) (n = 5), for 2, 4, and 6 h (Student unpaired t-test: **, $p < 0.01$; ***, $p < 0.001$). **E**: Locomotor activity of 5 dpf larvae exposed to either 15 μM DFP (n = 48) or vehicle (DMSO) (n = 48) (Mann-Whitney test: *, $p < 0.05$). **F**: Real-time measurement of oxygen consumption by 5 dpf larvae exposed to either 15 μM DFP or vehicle (DMSO). **G**: Quantification of oxygen consumption rate (OCR) of larvae exposed to either 15 μM DFP (n = 301) or vehicle (DMSO) (n = 189) (Student unpaired t-test: ***, $p < 0.001$). Abbreviations: Ey, eye; Br, brain; Ea, ear.

3.2 AChE inhibition, leading to paralysis and respiratory failure in DFP exposed larvae

As AChE inhibition and muscle paralysis are hallmarks of OP poisoning, we measured the motor activity of DFP-exposed and control larvae, by measuring the distance swum by these individuals over a 30-min period. As expected, larvae exposed to DFP (n = 48) showed significantly decreased motor activity compared to their control siblings (n = 48) (Figure 1D). We next estimated AChE activity in larvae exposed to either 15 μM DFP (n = 5) or vehicle (DMSO 1%) (n = 5). We observed a 50% inhibition of AChE activity as early as 2 h after DFP exposure (Figure 1E). As respiratory failure is an early consequence of OP poisoning[28,29], we next quantified the respiration of larvae exposed to 15 μM DFP by calculating the extracellular oxygen consumption rate (ORC) of living larvae using the MitoXpress Xtra oxygen consumption assay, a simple kinetic measurement of oxygen consumption (Figure 1F). Results showed that the OCR of

larvae exposed to 15 μM DFP were 88.78 ± 1.00% of that observed in controls (Figure 1G, $p <$ 0.001). Thus, after DFP exposure, zebrafish larvae displayed strong inhibition of AChE activity, decreased oxygen consumption, and reduced motor activity.

3.3 DFP exposure promoted neuronal hyperexcitation and apoptosis

Increase in c-Fos expression, a molecular marker of activity, is observed during seizures[30], and has been shown to promote epileptogenesis[31–34]. As a first attempt to evaluate the consequences of DFP poisoning on neuronal activity, we studied c-Fos expression in DFP-treated and control sibling larvae. Interestingly, qRT-PCR revealed a significant increase in c-Fos mRNA accumulation following DFP poisoning (Figure 2B, $p < 0.001$), suggesting increased neuronal excitation. We then sought to visualize neuronal activity in live brains of larvae exposed to DFP using calcium imaging. Indeed, transient calcium uptakes in neurons, as revealed by GCaMP5G fluorescent protein, fully correlates neuronal excitation in zebrafish epilepsy models, allowing to visualize seizures in vivo at the level of a whole brain[11,35]. Five dpf larvae from the transgenic line Tg[Huc:GCaMP5G] were treated with DFP and neuronal activity was recorded during the 6 h of incubation time using time-lapse confocal microscopy (Figure 2E, and supplementary video 2). As early as 20 min following DFP addition, some intense transient calcium uptake events were detected; their number and intensity progressively increased over the next 2 hours (Figure 2F, G). Then, 2 - 3 hours following DFP addition, all DFP-treated larvae (n = 5) displayed massive, brief and synchronous calcium uptake events in both neuropils of the optic tectum neurons, strongly reminiscent of those seen during generalized seizures in zebrafish epilepsy models (Figure 2C2).

To confirm that the increase in neuronal calcium uptakes observed in DFP-exposed larvae did correspond to actual neuronal hyperexcitation, we ascertained whether administration of

diazepam, the main drug administered to epileptic patients to relieve seizures[36], alleviated calcium uptake activity. Larvae were first exposed to DFP (15 μM) for 5 h, and their neuronal calcium activity was recorded for 30 minutes; diazepam (40 μM) was then added and their neuronal calcium activity was recorded for an additional 60 min. Interestingly, exposure to diazepam significantly decreased neuronal excitation induced by DFP (Figure 2H, I). All these data confirm that DFP exposure caused an intense neuronal hyperexcitation.

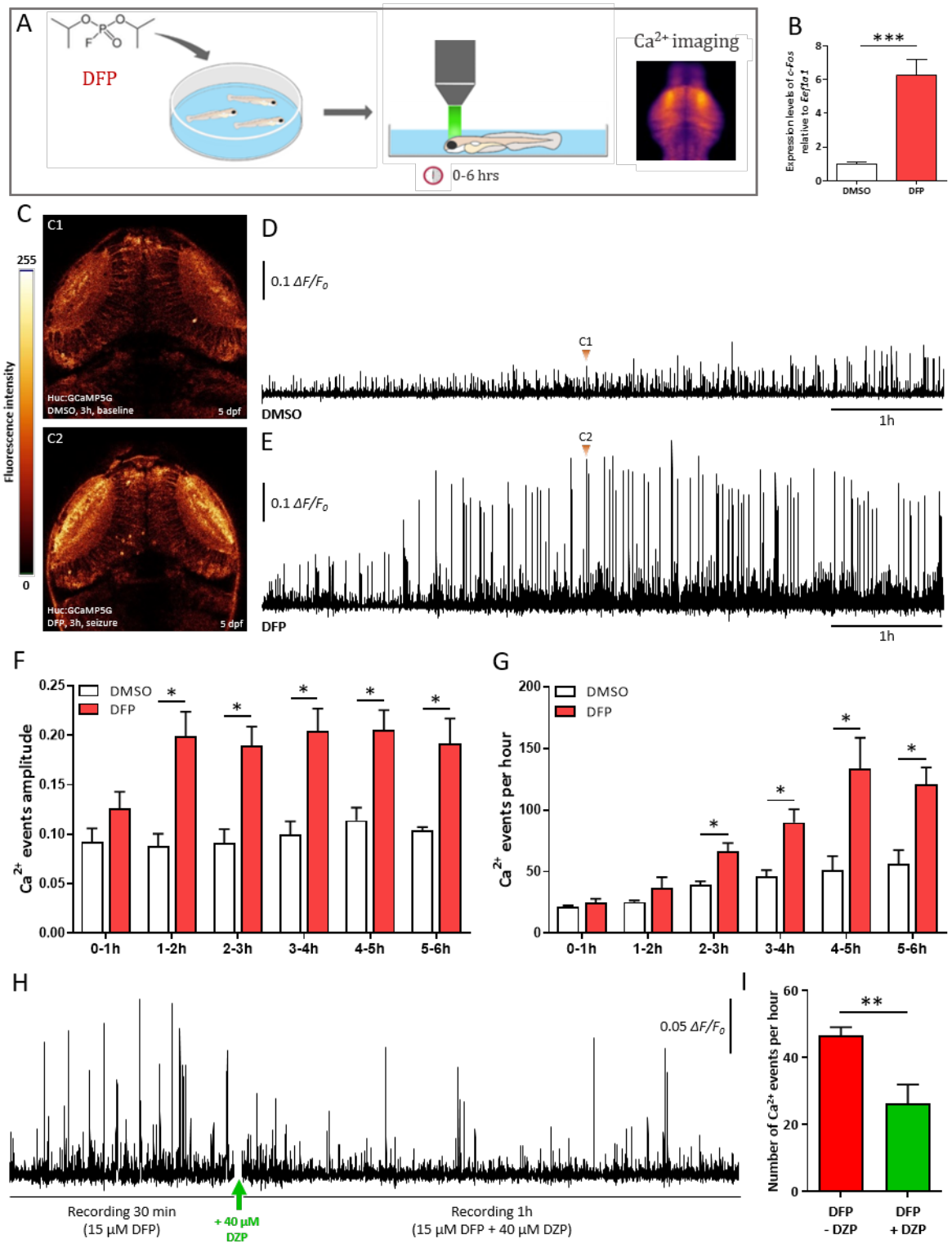

Figure 2. DFP exposure caused increased neuron excitation. **A**: In the experimental set-up, 5 dpf Tg[Huc:GCaMP5G] larvae were exposed to either 15 μM DFP or vehicle (DMSO), and transient

calcium uptakes were then recorded in brain neurons over 6 h using calcium imaging. **B**: qRT-PCR demonstrated markedly increased expression of the *C-Fos* gene in larvae exposed to 15 μM DFP (n = 19) when compared to that in control larvae (DMSO) (n = 19) (Student unpaired t-test: ***, $p < 0.001$). **C**, Snapshot views of calcium imaging of 5 dpf Tg[Huc:GCaMP5G] larvae brain showing baseline calcium activity (C1 in Figure 2D) and seizure-like hyperactivity (C2 in Figure 2E) seen 3 h after 15 μM DFP exposure. **D**: Transient calcium uptakes in 5 dpf Tg[Huc:GCaMP5G] larvae treated with vehicle (DMSO) (n = 5). **E**: Transient calcium uptakes in 5 dpf Tg[Huc:GCaMP5G] larvae exposed to 15 μM DFP (n = 5). **F**: Amplitude of calcium uptake events in 5 dpf Tg[Huc:GCaMP5G] larvae at different time points during exposure to either 15 μM DFP (n = 5) or vehicle (DMSO) (n = 5) (Student unpaired t-test: *, $p < 0.05$). **G**: Number of calcium uptake events showing $\Delta F/F_0 > 0.04$ in 5 dpf Tg[Huc:GCaMP5G] larvae at different time points during exposure to either 15 μM DFP (n = 5) or vehicle (DMSO) (n = 5) (Student unpaired t-test: *, $p < 0.05$). **H**: Pattern of transient calcium uptake events in 5 dpf Tg[Huc:GCaMP5G] larvae exposed to 15 μM DFP for 5 h and then to 15 μM DFP + 40 μM diazepam (DZP) for one more hour. **I**: Number of calcium uptake events showing $\Delta F/F_0 > 0.04$ in 5 dpf Tg[Huc:GCaMP5G] larvae exposed to either 15 μM DFP or 15 μM DFP + 40 μM diazepam (DZP) (Student unpaired t-test: $p = 0.009$).

Exposure to highly toxic OP compounds (soman, sarin, VX) has been shown to cause elevated neuronal loss in both humans and animal models[24,37–40]. We thus examined whether the larvae exposed to DFP showed an increase in neuronal death. Using acridine orange (AO), a vital marker that labels dying cells, we first observed in living larvae a marked increase in the number of cells showing AO staining in DFP-exposed larvae compared to controls (Figure 3C, D, E). Anti-

306 activated-caspase-3 immunolabeling confirmed that DFP exposure promotes neuronal apoptosis
307 (Figure 3F, G, H).

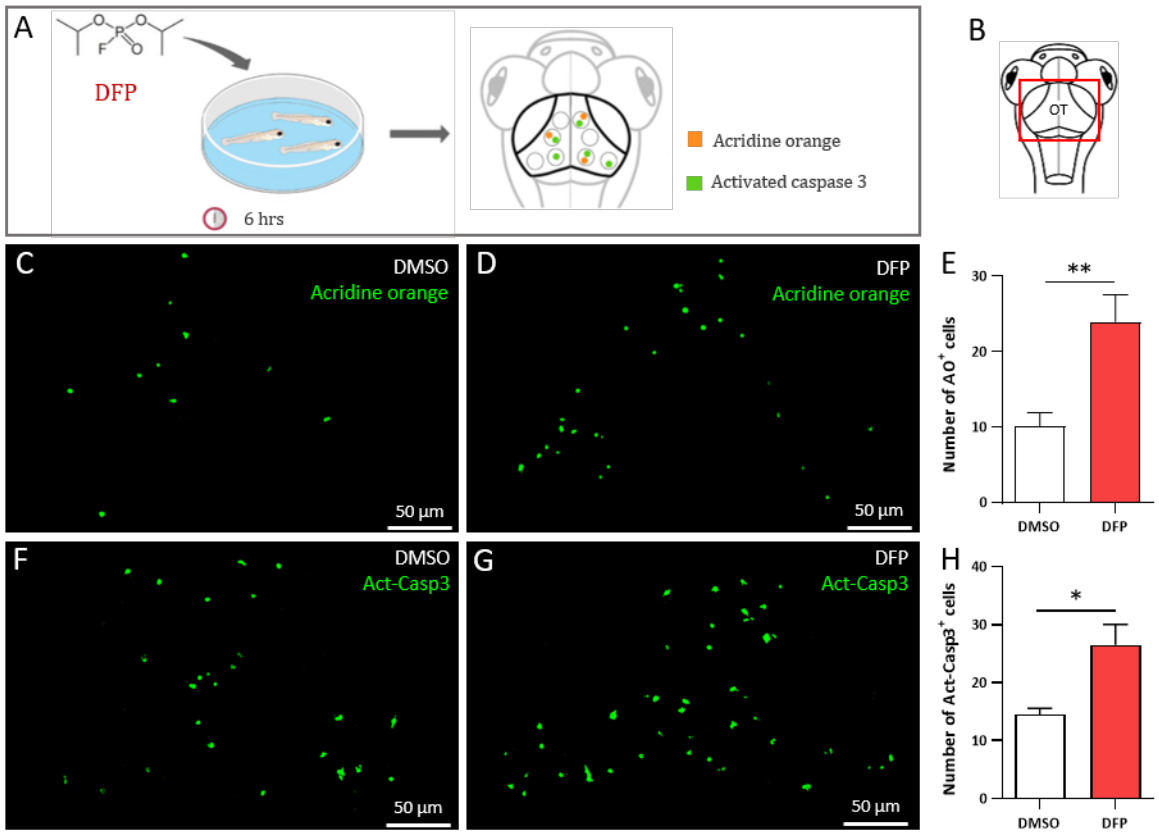

308

309 **Figure 3.** DFP exposure promoted increased neuron apoptosis. **A**: In the experimental set-up, 5 dpf
310 larvae were exposed to either 15 μM DFP or vehicle (DMSO) for 6 h, prior to acridine orange
311 staining or anti-activated caspase-3 immunolabeling. **B**: Scheme of 5 dpf larvae head with the red
312 box showing the region of interest in the brain uncovering the optic tectum (OT). **C** and **D**: Acridine
313 orange labeling of dead neuronal cells in 5 dpf larvae exposed for 6 h to either vehicle (DMSO)
314 (C) or 15 μM DFP (D). Scale bar: 50 μm. **E**: Number of acridine orange-positive cells in 5 dpf
315 larvae exposed for 6 h to either vehicle (DMSO) (n = 8) or 15 μM DFP (n = 10) (Student unpaired
316 t-test: p = 0.002). **F** and **G**: Anti-activated caspase-3 (Act-Casp3) immunolabeling of dying
317 neuronal cells in 5 dpf larvae exposed for 6 h to either vehicle (DMSO) (F) or 15 μM DFP (G).

Scale bar: 50 μm. **H**: Number of activated-caspase-3 positive cells in 5 dpf larvae exposed for 6 h to either vehicle (DMSO) (n = 7) or 15 μM DFP (n = 8) (Student unpaired t-test with Welch's correction: p = 0.01).

3.5 Increased NR2B-NMDA receptor expression and decreased GAD65/67 and gephyrin protein accumulation in DFP exposed larvae

It has been shown that following OP exposure, AChE inhibition causes an acute stimulation of cholinergic receptors, inducing increased neuronal glutamatergic response, and excessive NMDA receptor activation[41–43]. To examine whether accumulation of the NR2B-NMDA receptor sub-unit, a major excitatory glutamate receptor, was affected following DFP exposure, brain sections of larvae exposed to DFP and control siblings were analyzed by immunocytochemistry using an anti-NR2B-NMDA receptor antibody (Figure 4A, excitatory synapse). Interestingly, results showed a clear increase in NR2B-NMDA accumulation in the brains of DFP-exposed larvae, compared to untreated controls (Figure 4C, Supplementary video 3 and 4). The increased NR2B-NMDA accumulation induced by DFP poisoning was confirmed by quantification of NR2B-NMDA staining using Imaris software (Bitplane Inc., Version 9.1.2) (Figure 4G). To further characterize neuronal networks in DFP-treated larvae, we analyzed the accumulation of glutamate decarboxylase (GAD65/67), an enzyme involved in GABA synthesis in presynaptic inhibitory synapses, and gephyrin, a protein that anchors postsynaptic GABA receptors to the cytoskeleton, using anti-GAD65/67 and anti-gephyrin antibodies, respectively (Figure 4A, inhibitory synapse). Interestingly, following DFP exposure, we observed a significant decrease in the accumulation of both GAD65/67 (Figure 4D) and gephyrin (Figure 4F). Labeling quantification using Imaris

339 software (Bitplane Inc., Version 9.1.2) confirmed the decreased accumulation of both GAD65/67
340 (Figure 4H) and gephyrin in DFP-treated larvae (Figure 4I).

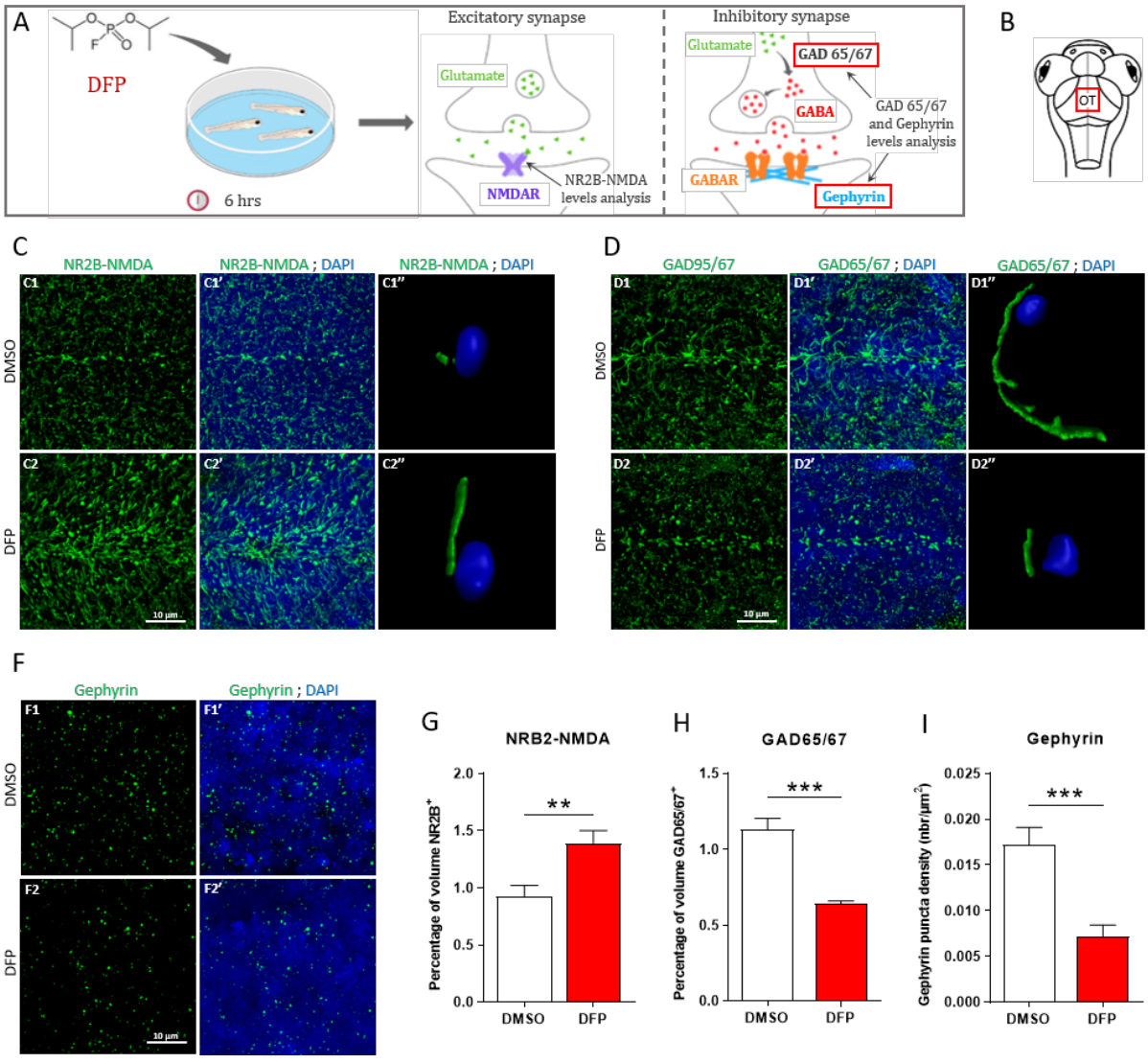

341

342 **Figure 4.** DFP exposure provoked increased NR2B-NMDA receptor accumulation. **A**: As
343 experimental set-up, 5 dpf larvae were exposed to either 15 μM DFP or vehicle (DMSO) for 6
344 hours, prior to NR2B-NMDA immunolabelling of glutamatergic/excitatory synapses. **B**: Scheme
345 of 5 dpf larvae head with the red box showing the region of interest in the brain uncovering the
346 optic tectum (OT). **C**: Anti-NR2B-NMDA receptor immunolabelling of glutamatergic synapses

(C1 to C2') and DAPI staining (C1', C2') in 5 dpf larvae exposed for 6 hours to either vehicle (DMSO) (C1, C1') or 15 μM DFP (C2, C2'). Scale bar: 10 μm. 3D image reconstruction of NR2B-NMDA labeled neuron branch details in 5 dpf larvae exposed for 6 hours to either vehicle (DMSO) (C1'') or 15 μM DFP (C2''). **D**: Anti-GAD 65/67 immunolabeling of GABAergic presynapses (D1 to D2') and DAPI staining (D1', D2') in 5 dpf larvae exposed for 6 h to either vehicle (DMSO) (D1, D1') or 15 μM DFP (D2, D2'). Scale bar: 10 μm. D, 3D image reconstruction of GAD 65/67 labeled neuron branch details in 5 dpf larvae exposed for 6 h to either vehicle (DMSO) (D1'') or 15 μM DFP (D2''). **F:** Anti-gephyrin immunolabeling of GABAergic presynapses (F1 to F2') and DAPI staining (F1', F2') in 5 dpf larvae exposed for 6 h to either vehicle (DMSO) (F1, F1') or 15 μM DFP (F2, F2'). Scale bar: 10 μm. **G**: Quantification of the volume of NR2B-NMDA labeled branch material in 5 dpf larvae treated for 6 hours with either vehicle (DMSO) (n = 13) or 15 μM DFP (n = 13) (Student unpaired t-test: p = 0.004). **H**: Quantification of the volume of GAD 65/67 labeled branch material in 5 dpf larvae treated for 6 h with either vehicle (DMSO) (n = 14) or 15 μM DFP (n = 14) (Student unpaired t-test with Welch's correction: ***, $p < 0.001$). **I**: Quantification of the density of gephyrin puncta in 5 dpf larvae treated for 6 h with either vehicle (DMSO) (n = 20) or 15 μM DFP (n = 20) (Mann-Whitney: ***, $p < 0.001$).

4. DISCUSSION

Because of their use for agricultural purposes worldwide, acute poisoning by OP compounds is a major public health problem, with several millions of intoxications reported each year[44,45]. In this work, we took advantage of the possibilities offered by zebrafish larvae to develop an animal model of OP poisoning and study the consequences of OP exposure on neuronal network activity. Interestingly, as described in mammalian models of OP poisoning[46,47], zebrafish larvae

exposed to DFP displayed marked AChE inhibition, the hallmark of OP intoxication, validating this small fish as a good model for investigating the consequences of OP poisoning. One of the most devastating features of OP intoxication in both humans and rodents is full, sometimes fatal, respiratory failure[28]. It is important to note that in epileptic OP intoxication models that use mammals, the induced respiratory failure must be prevented by the simultaneous addition of cholinergic inhibitors (atropine) and AChE reactivators (oximes) to avoid premature death[29]. By contrast, although we observed that DFP-treated larvae showed significantly decreased oxygen consumption, there was no need to protect larvae with cholinergic inhibitors. Thus, DFP-exposed zebrafish larvae appeared as a powerful and simple model to test the effects of anti-convulsive agents in absence of either muscarinic antagonists or cholinesterase reactivators.

It has been demonstrated that acute OP exposure causes epileptic-like seizures, which, if not treated, can eventually lead to life-threatening status epilepticus[47]. We therefore investigated neuronal excitation in larvae exposed to DFP. We first found that larvae exposed to DFP showed increased expression of c-Fos, a marker of neuronal activity, which is overexpressed after seizures[48–50]. We next recorded neuronal calcium uptakes in living larvae exposed to DFP, a technology that enables visualization of epileptic seizures[11,35]. In DFP-exposed larvae, as early as 20 minutes following OP addition, we observed neurons showing massive calcium uptake events that were never seen in control siblings, and which number increased over the next 2 h. Moreover, the OP-induced neuronal activity was potently alleviated by diazepam treatment, confirming that larvae exposed to DFP show neuronal hyperexcitation reflecting epileptiform seizures. In humans, if victims are not treated within the first 30 minutes, seizures caused by OP intoxication can end in status epilepticus, a major life-threatening neurologic disorder[6,51], also leading to long term brain damages[52,53]. This 30-minute long status epilepticus window frame also appears to be a critical

period during which long-term brain lesions are generated[51]. In the Tokyo subway attack, approximately 3% of OP-poisoned victims suffered convulsions[54]. Interestingly, 2 - 3 h after DFP exposure, we observed that all the DFP-exposed larvae showed massive synchronous calcium uptake events, strongly reminiscent of generalized seizures seen in zebrafish epilepsy models[11,35], suggesting that these larvae displayed a status epilepticus-like phenotype.

Together with AChE inhibition and neuronal seizures, massive neuronal death is another hallmark of OP poisoning[20], also observed in the DFP-exposed zebrafish larvae. At the cellular level, it has long been known that hyperactivity of cholinergic receptors induces a massive release of glutamate, leading to over-activation of glutamatergic receptors and neuronal hyperexcitability[41–43]. Specifically, it has been shown that acute OP intoxication induces the activation of NMDA receptors[55]. Moreover, in a mammalian model of OP poisoning, activation of NMDA receptors plays essential roles in seizure activity and apoptosis[52,56]. In the brain of zebrafish larvae exposed to DFP, we observed a decreased accumulation of both gephyrin and GAD65/67, two proteins specifically accumulated in inhibitory synapses, while NR2B-NMDA receptor was significantly overexpressed. This suggests that following acute DFP poisoning, neuronal hyperexcitation results from a shift in the synaptic balance of brain neurons toward excitatory states.

We report here a vertebrate model of OP poisoning that displays phenotypes and symptoms of acute toxicity, faithfully recapitulating those described in humans, i.e. AChE inhibition, respiratory deficit, neuronal apoptosis and epileptiform seizures. The zebrafish is thus a model of choice for large-scale screening of entities that could restore CNS functions after OP poisoning and mitigate the long-term neurological sequelae of acute OP poisoning in humans.

ACKNOWLEDGMENTS

We thank Christiane Romain (Inserm UMR 1141) and Olivier Bar (Inserm UMR 1141).

DISCLOSURE

The authors declare that the research was conducted in the absence of any commercial or financial relationships that could be construed as a potential conflict of interest.

SUPPLEMENTARY MATERIAL

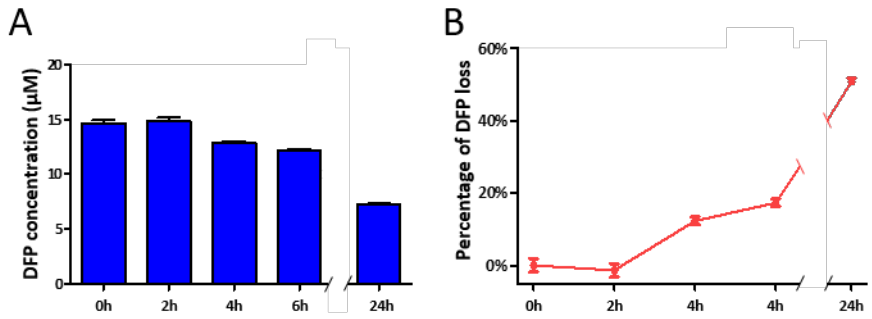

Figure S1. Monitoring the stability of DFP diluted in FW. A: Residual concentrations of DFP measured at different time points following dilution to 15 μM in FW. B: Percentage of DFP loss over time showing a 2% loss per hour, approximately.

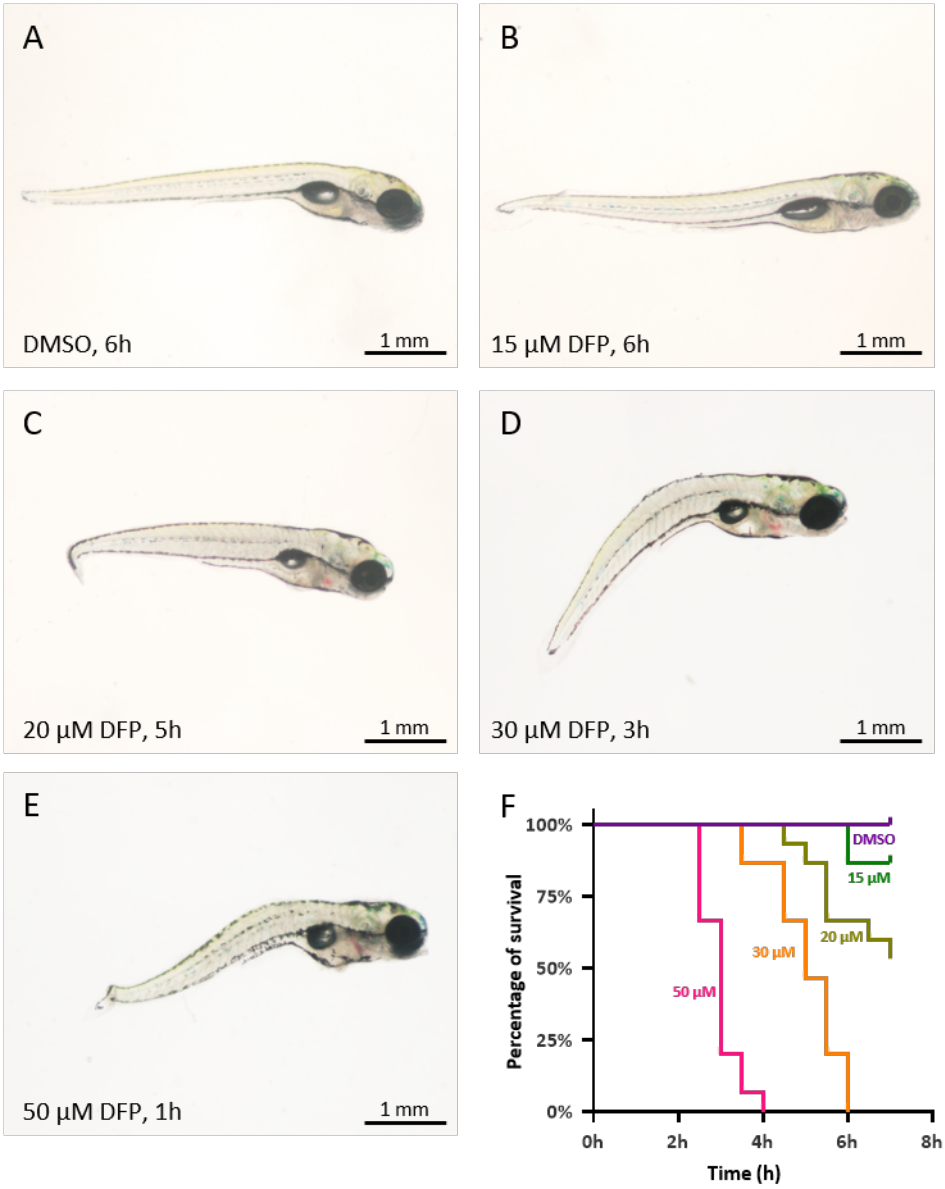

Figure S2. DFP exposure caused phenotypic defects and larval lethality. A-E: Phenotypes of 5 dpf larvae exposed to either vehicle (DMSO) for 6 h (A), or 15 μM DFP for 6 h (B), or 20 μM DFP for 5 h (C), or 30 μM DFP for 3 h (D), or 50 μM for 1 h (E). Scale bar: 1 mm. F: Survival curve of 5 dpf larvae exposed to either vehicle (DMSO) or 15, 20, 30 or 50 μM DFP.

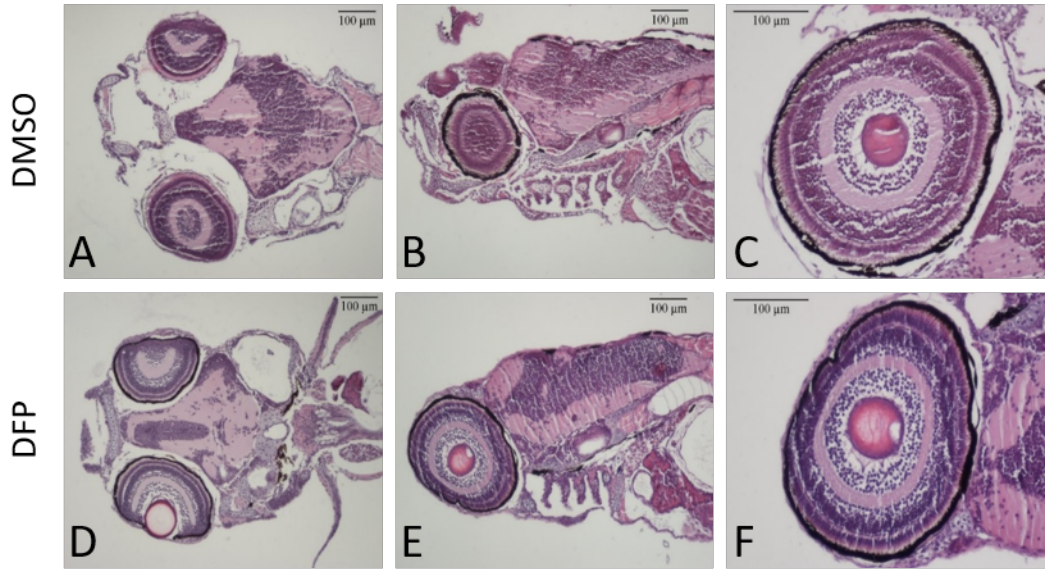

Figure S3. Zebrafish larvae exposed for 6 h to 15 μM DFP do not show visible phenotypic defects. A-F Horizontal (A, D) and sagittal (B, C, E, F) tissue sections of 5 dpf larvae (A, B, D, E) and corresponding eyes (C, F), following exposure for 6 h to either vehicle (DMSO) (A, B, C) or 15 μM DFP (D, E, F).

Supplementary Video 1. 3 minute-long representative recording of calcium activity imaging in optic tectum neurons of 5 dpf larvae following 3 h exposure to vehicle (DMSO). Movie played at 25 fps.

Supplementary Video 2. 3 minute-long representative recording of calcium activity imaging in optic tectum neurons of 5 dpf larvae following 3 h exposure to 15 μM DFP. Movie played at 25 fps.

Supplementary Video 3. 3D reconstruction of the image depicted in Figure 4C1', showing the optic tectum from a 5 dpf larva exposed for 6 hto vehicle (DMSO) and labeled with an anti-NR2B-NMDA antibody (green) and counterstained with DAPI (blue). 3D images were generated using Imaris software (Bitplane Inc., Version 9.1.2).

444 **Supplementary Video 4.** 3D reconstruction of the image depicted in Figure 4C2', showing the
445 optic tectum from a 5 dpf larva exposed for 6 h to 15 μM DFP and labeled with an anti-NR2B-
446 NMDA antibody (green) and counterstained with DAPI (blue). 3D images were generated using
447 Imaris software (Bitplane Inc., Version 9.1.2).

448 **Supplementary Video 5.** 3D reconstruction of the image depicted in Figure 5C1', showing the
449 optic tectum from a 5 dpf larva exposed for 6 h to vehicle (DMSO) and labeled with an anti-GAD
450 65/67 antibody (green) and counterstained with DAPI (blue). 3D images were generated using
451 Imaris software (Bitplane Inc., Version 9.1.2).

452 **Supplementary Video 6.** 3D reconstruction of the image depicted in Figure 5C2', showing the
453 optic tectum from a 5 dpf larva exposed for 6 h to 15 μM DFP and labeled with an anti-GAD 65/67
454 antibody (green) and counterstained with DAPI (blue). 3D images were generated using Imaris
455 software (Bitplane Inc., Version 9.1.2).

456 **Funding**: This work was supported by Institut National de la Santé et la Recherche Médicale
457 (INSERM), the Centre National de la Recherche Scientifique (CNRS), the French National
458 Research Agency (ANR-16-CE18-0010), and Fondation NRJ (Institut de France), and the Agence
459 de l'Innovation de Défense. Funding sources had no involvement in study design, collection,
460 analysis or interpretation of data, or decision to publish.

461 **Author Contributions**: A.B., performed the experiments, the analysis, and designed the figures.
462 N.S.Y. supervised the project and wrote the manuscript. J.S., performed the respiratory
463 experiments, R.H.A., R.L, M.P., A.I., D.S., and N.T. helped carry out the experiments .N.D. helped
464 supervise the project. C.Y. G.D.B., F.N., N.D, contributed to the final manuscript.

REFERENCES:

1. Mew EJ, Padmanathan P, Konradsen F, et al. The global burden of fatal self-poisoning with pesticides 2006-15: Systematic review. *J Affect Disord*. 2017;219(May):93-104. doi:10.1016/j.jad.2017.05.002

2. Konickx LA, Worek F, Jayamanne S, Thiermann H, Buckley NA, Eddleston M. Reactivation of Plasma Butyrylcholinesterase by Pralidoxime Chloride in Patients Poisoned by WHO Class II Toxicity Organophosphorus Insecticides. 2013. doi:10.1093/toxsci/kft217

3. Pereira EFR, Aracava Y, Detolla LJ, et al. Animal Models That Best Reproduce the Clinical Manifestations of Human Intoxication with Organophosphorus Compounds. *J Pharmacol Exp Ther J Pharmacol Exp Ther*. 2014;350:313-321. doi:10.1124/jpet.114.214932

4. Jett DA. Neurological aspects of chemical terrorism. *Ann Neurol*. 2007;61(1):9-13. doi:10.1002/ana.21072

5. Lotti M. Clinical Toxicology of Anticholinesterase Agents in Humans. In: *Hayes' Handbook of Pesticide Toxicology*. Elsevier Inc.; 2010:1543-1589. doi:10.1016/B978-0-12-374367-1.00072-0

6. Todorovic MS, Cowan ML, Balint CA, Sun C, Kapur J. Characterization of status epilepticus induced by two organophosphates in rats. *Epilepsy Res*. 2012;101(3):268-276. doi:10.1016/j.eplepsyres.2012.04.014

7. Chen Y. Organophosphate-induced brain damage: mechanisms, neuropsychiatric and neurological consequences, and potential therapeutic strategies. *Neurotoxicology*. 2012;33(3):391-400. doi:10.1016/j.neuro.2012.03.011

8. Collombet J-M. Nerve agent intoxication: Recent neuropathophysiological findings and subsequent impact on medical management prospects. 2011. doi:10.1016/j.taap.2011.07.003

9. Yanicostas C, Ernest S, Dayraud C, Petit C, Soussi-Yanicostas N. Essential requirement for zebrafish anosmin-1a in the migration of the posterior lateral line primordium. *Dev Biol*. 2008;320(2):469-479. doi:10.1016/j.ydbio.2008.06.008

10. Martin E, Yanicostas C, Rastetter A, et al. Spatacsin and spastizin act in the same pathway required for proper spinal motor neuron axon outgrowth in zebrafish. *Neurobiol Dis*. 2012;48(3):299-308. doi:10.1016/j.nbd.2012.07.003

11. Brenet A, Hassan-Abdi R, Somkhit J, Yanicostas C, Soussi-Yanicostas N. Defective Excitatory/Inhibitory Synaptic Balance and Increased Neuron Apoptosis in a Zebrafish

Model of Dravet Syndrome. *Cells*. 2019;8(10):1199. doi:10.3390/cells8101199

12. Ghoumid J, Drevillon L, Alavi-Naini SM, et al. ZEB2 zinc-finger missense mutations lead to hypomorphic alleles and a mild Mowat-Wilson syndrome. *Hum Mol Genet*. 2013;22(13):2652-2661. doi:10.1093/hmg/ddt114

13. Yanicostas C, Barbieri E, Hibi M, Brice A, Stevanin G, Soussi-Yanicostas N. Requirement for Zebrafish Ataxin-7 in Differentiation of Photoreceptors and Cerebellar Neurons. *PLoS One*. 2012;7(11). doi:10.1371/journal.pone.0050705

14. MacRae CA, Peterson RT. Zebrafish as tools for drug discovery. *Nat Rev | DRUG Discov*. 2015;14:721-731. doi:10.1038/nrd4627

15. Lessman CA. The developing zebrafish (Danio rerio): A vertebrate model for high-throughput screening of chemical libraries. *Birth Defects Res Part C - Embryo Today Rev*. 2011;93(3):268-280. doi:10.1002/bdrc.20212

16. Delvecchio C, Tiefenbach J, Krause HM. The Zebrafish: A powerful platform for in vivo, HTS drug discovery. *Assay Drug Dev Technol*. 2011;9(4):354-361. doi:10.1089/adt.2010.0346

17. Rinkwitz S, Mourrain P, Becker TS. Zebrafish: An integrative system for neurogenomics and neurosciences. *Prog Neurobiol*. 2011;93(2):231-243. doi:10.1016/j.pneurobio.2010.11.003

18. Ito H, Yamamoto N. Non-laminar cerebral cortex in teleost fishes? *Biol Lett*. 2009;5(1):117-121. doi:10.1098/rsbl.2008.0397

19. Wullimann MF. Secondary neurogenesis and telencephalic organization in zebrafish and mice: a brief review. *Integr Zool*. 2009;4(1):123-133. doi:10.1111/j.1749-4877.2008.00140.x

20. Flannery BM, Bruun DA, Rowland DJ, et al. Persistent neuroinflammation and cognitive impairment in a rat model of acute diisopropylfluorophosphate intoxication. *J Neuroinflammation*. 2016;13(1):1-16. doi:10.1186/s12974-016-0744-y

21. Li Y, Lein PJ, Liu C, et al. Spatiotemporal pattern of neuronal injury induced by DFP in rats: A model for delayed neuronal cell death following acute OP intoxication. *Toxicol Appl Pharmacol*. 2011;253(3):261-269. doi:10.1016/j.taap.2011.03.026

22. Auta J, Costa E, Davis J, Guidotti A. Imidazenil: a potent and safe protective agent against diisopropyl fluorophosphate toxicity. *Neuropharmacology*. 2004;46(3):397-403. doi:10.1016/j.neuropharm.2003.09.010

23. Deshpande LS, Carter DS, Blair RE, DeLorenzo RJ. Development of a Prolonged Calcium Plateau in Hippocampal Neurons in Rats Surviving Status Epilepticus Induced by the

Organophosphate Diisopropylfluorophosphate. *Toxicol Sci*. 2010;116(2):623-631. doi:10.1093/toxsci/kfq157

24. Kim YB, Hur GH, Shin S, Sok DE, Kang JK, Lee YS. Organophosphate-induced brain injuries: delayed apoptosis mediated by nitric oxide. *Environ Toxicol Pharmacol*. 1999;7(2):147-152. http://www.ncbi.nlm.nih.gov/pubmed/21781920. Accessed September 2, 2019.

25. Wright LKM, Liu J, Nallapaneni A, Pope CN. Behavioral sequelae following acute diisopropylfluorophosphate intoxication in rats: comparative effects of atropine and cannabinomimetics. *Neurotoxicol Teratol*. 2010;32(3):329-335. doi:10.1016/j.ntt.2009.12.006

26. McDonough JH, Shih TM. Neuropharmacological mechanisms of nerve agent-induced seizure and neuropathology. *Neurosci Biobehav Rev*. 1997;21(5):559-579. http://www.ncbi.nlm.nih.gov/pubmed/9353792. Accessed September 2, 2019.

27. Yamasue H, Abe O, Kasai K, et al. Human brain structural change related to acute single exposure to sarin. *Ann Neurol*. 2007;61(1):37-46. doi:10.1002/ana.21024

28. Giyanwani PR, Zubair U, Salam O, Zubair Z. Respiratory Failure Following Organophosphate Poisoning: A Literature Review. 2017. doi:10.7759/cureus.1651

29. Carey JL, Dunn C, Gaspari RJ. Central respiratory failure during acute organophosphate poisoning. *Respir Physiol Neurobiol*. 2013;189(2):403-410. doi:10.1016/j.resp.2013.07.022

30. Szyndler J, Maciejak P, Turzyńska D, et al. Mapping of c-Fos expression in the rat brain during the evolution of pentylenetetrazol-kindled seizures. *Epilepsy Behav*. 2009;16(2):216-224. doi:10.1016/j.yebeh.2009.07.030

31. Iryo Y, Matsuoka M, Igisu H. Suppression of pentylenetetrazol-induced seizures and c-fos expression in mouse brain by L-carnitine. *J Occup Health*. 2000;42(3):119-123. doi:10.1539/joh.42.119

32. Morgan JI, Cohen DR, Hempstead JL, Curran T. Mapping patterns of c-fos expression in the central nervous system after seizure. *Science (80-)*. 1987;237(4811):192-197. doi:10.1126/science.3037702

33. Clark M, Post RM, Weiss SR, Cain CJ, Nakajima T. Regional expression of c-fos mRNA in rat brain during the evolution of amygdala kindled seizures. *Brain Res Mol Brain Res*. 1991;11(1):55-64. doi:10.1016/0169-328x(91)90021-o

34. Burazin TCD, Gundlach AL. Rapid and transient increases in cellular immediate early gene and neuropeptide mRNAs in cortical and limbic areas after amygdaloid kindling seizures in the rat. In: *Epilepsy Research*. Vol 26. ; 1996:281-293. doi:10.1016/S0920-1211(96)00060-

35. Liu J, Baraban SC. Network Properties Revealed during Multi-Scale Calcium Imaging of Seizure Activity in Zebrafish. *eNeuro*. 2019;6(1):ENEURO.0041-19.2019. doi:10.1523/ENEURO.0041-19.2019

36. Verrotti A, Milioni M, Zaccara G. Safety and efficacy of diazepam autoinjector for the management of epilepsy. *Expert Rev Neurother*. 2014;15(2):127-133. doi:10.1586/14737175.2015.1003043

37. Petras JM. NEUROLOGY AND NEUROPATHOLOGY OF SOMAN-INDUCED BRAIN INJURY: AN OVERVIEW. *J Exp Anal Behav*. 1994;61(2):319-329. doi:10.1901/jeab.1994.61-319

38. Shih T-M, Duniho SM, Mcdonough JH. Control of nerve agent-induced seizures is critical for neuroprotection and survival. 2003. doi:10.1016/S0041-008X(03)00019-X

39. Kaur P, Radotra B, Minz RW, Gill KD. Impaired mitochondrial energy metabolism and neuronal apoptotic cell death after chronic dichlorvos (OP) exposure in rat brain. 2007. doi:10.1016/j.neuro.2007.08.001

40. Gunay N, Kose B, Demiryurek S, Ceylan NO, Sari I, Demiryurek AT. Protective effects of Y-27632 on acute dichlorvos poisoning in rats. *Am J Emerg Med*. 2010;28(3):268-274. doi:10.1016/j.ajem.2008.11.020

41. Lallement G, Carpentier P, Pernot-Marino I, Baubichon D, Collet A, Blanchet G. Involvement of the different rat hippocampal glutamatergic receptors in development of seizures induced by soman: an autoradiographic study. *Neurotoxicology*. 1991;12(4):655-664. http://www.ncbi.nlm.nih.gov/pubmed/1665552. Accessed November 20, 2019.

42. Lallement G, Carpentier P, Collet A, et al. Involvement of glutamatergic system of amygdala in generalized seizures induced by soman: comparison with the hippocampus. *C R Acad Sci III*. 1991;313(9):421-426. http://www.ncbi.nlm.nih.gov/pubmed/1836748. Accessed November 20, 2019.

43. Lallement G, Carpentier P, Collet A, Pernot-Marino I, Baubichon D, Blanchet G. Effects of soman-induced seizures on different extracellular amino acid levels and on glutamate uptake in rat hippocampus. *Brain Res*. 1991;563(1-2):234-240. doi:10.1016/0006-8993(91)91539-D

44. Dawson AH, Eddleston M, Senarathna L, et al. Acute human lethal toxicity of agricultural pesticides: A prospective cohort study. *PLoS Med*. 2010;7(10). doi:10.1371/journal.pmed.1000357

45. Bertolote JM, Fleischmann A, Eddleston M, Gunnell D. Deaths from pesticide poisoning: a

global response. *Br J Psychiatry*. 2006;189(3):201-203. doi:10.1192/bjp.bp.105.020834

46. McCarren HS, McDonough JH. Anticonvulsant discovery through animal models of status epilepticus induced by organophosphorus nerve agents and pesticides. *Ann N Y Acad Sci*. 2016;1374(1):144-150. doi:10.1111/nyas.13092

47. Todorovic M, Cowan M, Balint C, Sun C, Kapur J. Characterization of status epilepticus induced by two organophosphates in rats. 2012. doi:10.1016/j.eplepsyres.2012.04.014

48. Dragunow M, Robertson HA. Kindling stimulation induces c-fos protein(s) in granule cells of the rat dentate gyrus. *Nature*. 1987;329(6138):441-442. doi:10.1038/329441a0

49. Le Gal G, Salle L. *Long-Lasting and Sequential Increase of c-Fos Oncoprotein Expression in Kainic Acid-Induced Status Epilepticus*. Vol 88.; 1988.

50. Simler S, Hirsch E, Danober L, Motte J, Vergnes M, Marescaux C. C-fos expression after single and kindled audiogenic seizures in Wistar rats. *Neurosci Lett*. 1994;175(1-2):58-62. doi:10.1016/0304-3940(94)91077-4

51. Trinka E, Cock H, Hesdorffer D, et al. A definition and classification of status epilepticus - Report of the ILAE Task Force on Classification of Status Epilepticus. *Epilepsia*. 2015;56(10):1515-1523. doi:10.1111/epi.13121

52. Shih TM, McDonough JH. Neurochemical mechanisms in soman-induced seizures. *J Appl Toxicol*. 1997;17(4):255-264. doi:10.1002/(SICI)1099-1263(199707)17:4<255::AID-JAT441>3.0.CO;2-D

53. Tryphonas L, Clement JG. Histomorphogenesis of soman-induced encephalocardiomyopathy in Sprague- Dawley rats. *Toxicol Pathol*. 1995;23(3):393-409. doi:10.1177/019262339502300316

54. Okumura T, Takasu N, Ishimatsu S, et al. Report on 640 victims of the Tokyo subway sarin attack. *Ann Emerg Med*. 1996;28(2):129-135. doi:10.1016/S0196-0644(96)70052-5

55. Kaur S, Singh S, Chahal KS, Prakash A. Potential pharmacological strategies for the improved treatment of organophosphate-induced neurotoxicity. *Can J Physiol Pharmacol*. 2014;92(11):893-911. doi:10.1139/cjpp-2014-0113

56. Solberg Y, Belkin M. The role of excitotoxicity in organophosphorous nerve agents central poisoning. *Trends Pharmacol Sci*. 1997;18(6):183-185. doi:10.1016/S0165-6147(97)89540-5